Progress In Electromagnetics Research C, Vol. 105, 241–251, 2020

Compact Triple-Band CPW-Fed Square Slot Antenna with Dual-Polarization Characteristics for Wireless Applications

Ting Wu[1], Juan Chen, and Peng-Fei Wu

Abstract—In this paper, a compact triple-band coplanar waveguide (CPW)-fed patch antenna with dual-polarization characteristics for wireless applications is proposed. The antenna is composed of an F-shaped patch, a grounded-C strip, a rectangular strip, and a horizontal rectangular grounded slot. The first circular polarized band is obtained by the F-shaped feed-line, and the second is achieved by the left C-shaped strip, while the right rectangle strip is responsible for the lower linearly polarized band. By inserting a slot at the right of the square slot, a notched band centered at 5.5 GHz is achieved. Both simulated and experimental results show that the antenna can generate three separate impedance bandwidths to cover frequency bands of 2.4/5.2/5.8-GHz WLAN band and X band. And the antenna is circularly polarized in the 5.8 GHz and 10 GHz band. Furthermore, the antenna structure is extremely simple and occupies small space. The proposed antenna has its applications in compact and portable devices operating at multiple frequency bands like cellular phones, Tablets, Wi-Fi devices, etc.

1. INTRODUCTION

Recently, the demand for antennas with multiband operation has increased since such antennas are vital for combining multiple communications standards in a single compact wireless system [1]. Planar antennas have been widely used due to the advantages of low profile, easy integration, and low fabrication cost [2, 3]. Many researchers have investigated several procedures to achieve multiband antennas, such as frequency-selective surface (FSS) [4–6] and electromagnetic band-gap (EBG) structure [7–9]. Among the well-known multiband antenna prototypes, CPW-fed antennas have become popular because they have many pleasing features such as no soldering point, easy fabrication, and a simplified configuration with a single metallic layer [10, 11]. Also, circularly polarized (CP) antennas are widely used in WLAN and satellites applications to enhance the polarization efficiency of the link budget [12–14]. Thus, multi-band linear and circular polarization performance is required in a single antenna. Various tri-band CPW-fed antennas [15–17] have been presented in recent years. However, these antennas can achieve either tri-band or circular polarization, not both of them. Furthermore, these antennas are somewhat complicated in their structure which limits their availability for practical applications. Moreover, the coexisting narrow-band applications can affect the performance of UWB systems. So we should avoid the interferences for better performance of the systems. Band-stop filer can be used to avoid interference with the increase of cost and complexity of the system. A better way to avoid interference is using UWB antenna with band-notch characteristic. Various UWB antennas with band-notch characteristics have been reported in the last few years, such as etching different slots, adding circuit stub, and using metamaterial resonator [18]. Using these techniques, many antennas have been reported to achieve single notch band [19], dual band notch [20], and triple notch band [21]. Multiband antennas have become more popular nowadays due to high demand for multi-functionality and improved date rate with the advancement in wireless communication technology. It would be particularly interesting

Received 27 May 2020, Accepted 9 September 2020, Scheduled 29 September 2020
* Corresponding author: Ting Wu (wutingzdh@xaut.edu.cn).
The authors are with the Xi'an University of Technology, Xi'an, Shaanxi 710048, People's Republic of China.

to use it in a compact hybrid coaxial architecture for UWB quasi-optical power combiners [22] in Bluetooth/WiMAX/WLAN applications [23–25] and in WPAN applications [26].

In this paper, a novel triple-band CPW-fed patch antenna with dual-polarization characteristics is proposed. The antenna is composed of an F-shaped patch, a grounded-C strip, a rectangular strip, and a horizontal rectangular grounded slot which consists of a C-shaped strip and a rectangle strip with a slot inserted in the opposite of the substrate at the center of the square slot. The antenna is fabricated and tested. The results show that the antenna has three separate operation bands ranging from 2.28–3.11 GHz, 4.12–7.43 GHz, and 8.45–11.42 GHz, which can cover the 2.4/5.8 GHz WLAN band and X-band. In addition, the antenna is circularly polarized in the two bands centred at 5.8 GHz and 10 GHz, respectively. Moreover, the antenna is extremely simple which manifests the suitability of the proposed antenna for the wireless applications. Detailed geometry configuration and experimental results of the proposed antenna are demonstrated in the following parts. Antenna design, CP mechanism, and parametric study are discussed in Section 2. In Section 3, the experimental results and discussion are presented. At last, the work is concluded.

2. STRUCTURE DESIGN AND ANALYSIS

2.1. Geometry Configuration of the Proposed Antenna

The proposed triple-band coplanar waveguide (CPW)-fed patch antenna with dual-polarization characteristics is shown in Figure 1. The antenna is fabricated on a single-layer FR4 substrate with a relative dielectric constant of 4.4, loss tangent of 0.02, and thickness of 0.8 mm. The overall dimension of the antenna is only $40 \times 40\,\text{mm}^2$. The antenna is composed of an F-shaped patch, a grounded-C strip, a rectangular strip, and a horizontal rectangular grounded slot. The first circularly polarized band is obtained by the F-shaped feed-line, and the second is achieved by the left C-shaped strip, while the right rectangle strip is responsible for the lower linearly polarized band. By inserting a slot at the right of the square slot, a notched band is achieved. The numerical analysis and geometry refinement of the proposed antenna are performed by using ANSYS HFSS 13.0 simulation software. The final optimized dimensions are listed in Table 1.

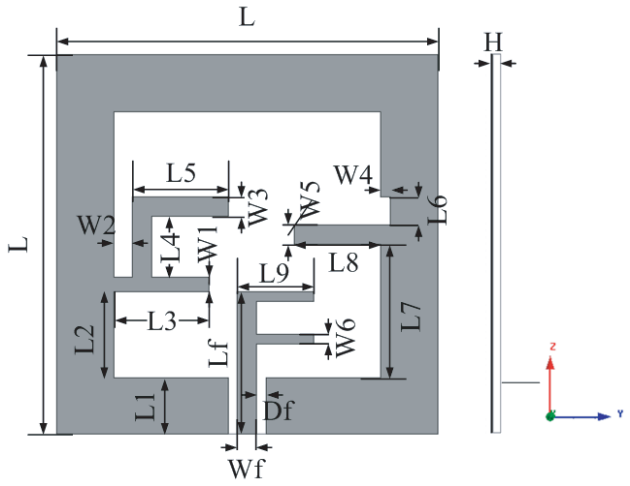

Figure 1. Configuration of the proposed antenna.

2.2. Evolution Process of the Antenna

To better understand the design processes and the contribution of individual element, Figure 2 shows the six evolution stages of the antenna. The six structures with different elements are simulated to make it more intuitive, and the simulated results of the different antennas are show in Figure 3. As shown in Figure 2, we can clearly see that Antenna 1 is a simple CPW-fed antenna which shows wide impedance

Table 1. Parameters for the proposed antenna (unit: mm).

L	$L1$	$L2$	$L3$	$L4$
40	9	6.5	10	6.5
$L5$	$L6$	$L7$	$L8$	$L9$
10	3	14	9	8
Lf	$W1$	$W2$	$W3$	$W4$
15	1.5	2	2	1
$W5$	$W6$	Wf	Df	
2	1	2	1	

bandwidth with linear polarization (LP). And the feed structure is rectangle. In the second stage, the feed structure is improved to F-shape as shown in Antenna 2. The impedance bandwidth decreases while the circularly polarized band ranging from 6.27 to 6.78 GHz is obtained. Then, a rectangle strip is embedded at the right part of the ground plane to constitute Antenna 3. Antenna 3 supports two operating bands. Based on Antenna 3, a C-shaped strip is introduced to obtain Antenna 4. We can see that it still shows two operating bands while the AR of the upper band is improved nearly to 3 dB. This indicates that the second circularly polarized band is formulated gradually. By introducing a rectangle strip at the left part of the ground plane, Antenna 5 is formed. The operating band ranging from 2.29 to 3.21 GHz can be obtained. Meanwhile, a broad bandwidth from 4.22 to 13.23 GHz is also obtained which means the waste of bandwidth. To achieve the requirement we wanted, a slit is embedded at the right of the ground plane in the last stage. A notched band is created to provide triple-band characteristics in Antenna 6. By combining the structures together and carefully adjusting the elements, the proposed antenna can work in three frequency bands with dual-polarization characteristics.

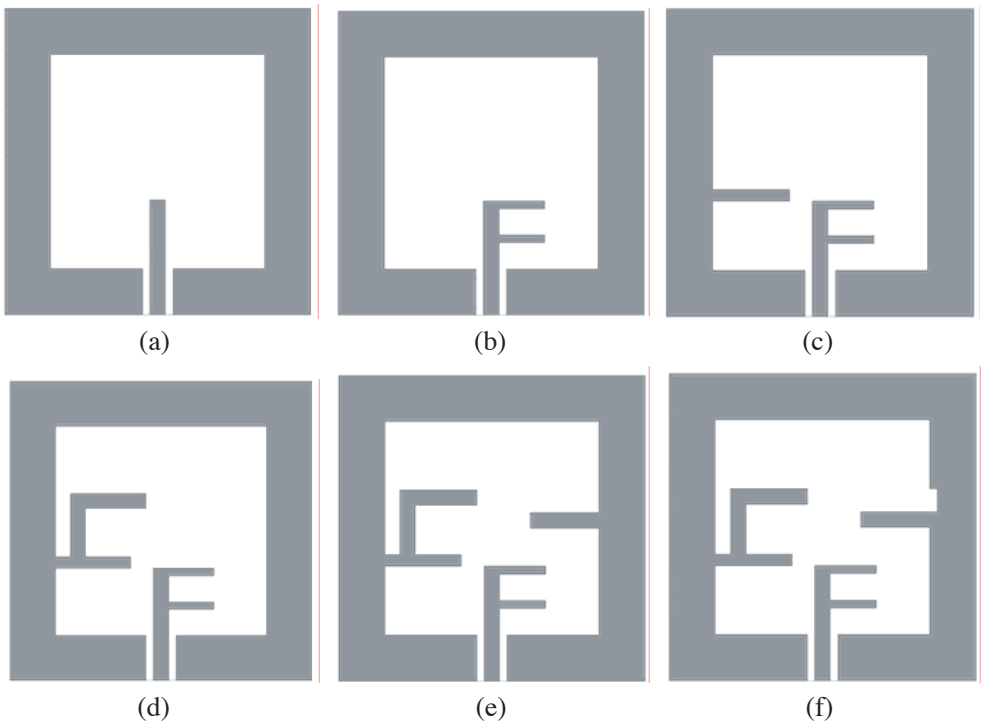

Figure 2. Evolution process of the proposed antenna. (a) Antenna 1. (b) Antenna 2. (c) Antenna 3. (d) Antenna 4. (e) Antenna 5. (f) Antenna 6.

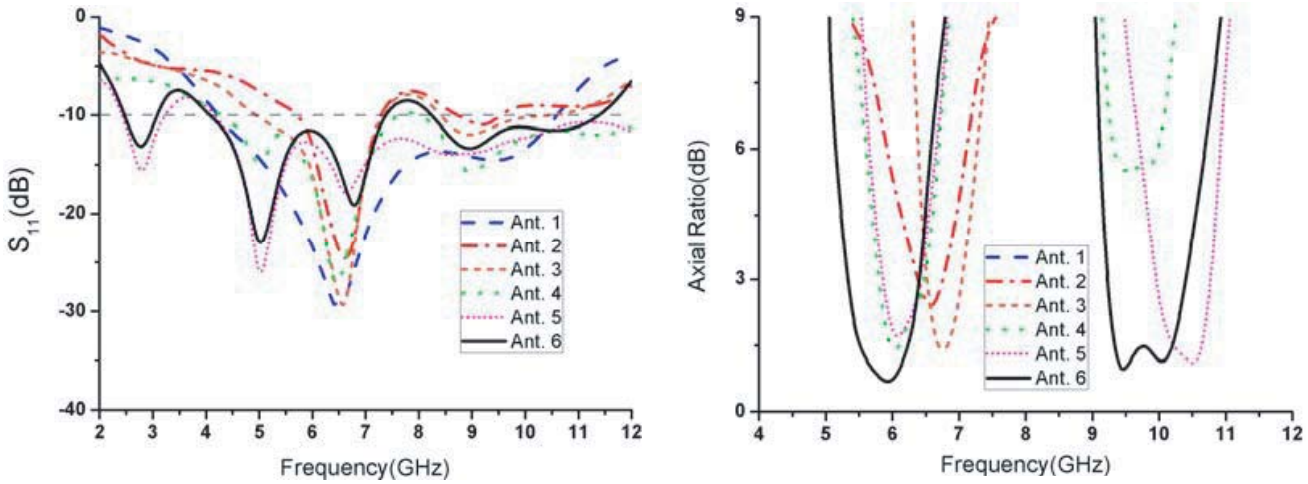

Figure 3. Simulated results of the different antennas. (a) Reflection coefficient. (b) Axial ratio.

The frequency of the notched band can be adjusted by changing the length of the slit embedded at the right of the ground plane $L6$. And the slot is about half of guided wavelength at the required notch band. The notch frequency f_n can be calculated by the following two equations as:

$$f_n = \frac{c}{2L\sqrt{\varepsilon_{reff}}} \tag{1}$$

$$\varepsilon_{reff} \approx \frac{\varepsilon_r + 1}{2} \tag{2}$$

where ε_{reff} is the effective dielectric constant, and c is the speed of light. The desired notch bandwidth can be obtained by adjusting the length of the slot. IBW and 3-dB ARBW of the six antennas are shown in Table 2. We can clearly see that the proposed antenna (Antenna 6) can generate three separate impedance bandwidths to cover frequency bands of 2.4/5.2/5.8 GHz WLAN band and X band. And the antenna is circularly polarized in the 5.8 GHz and 10 GHz band.

Table 2. Comparisons of IBWS and ARBW of the different antennas.

Antenna configuration	Bandwidth (GHz)	3-dB ARBW (GHz)	Antenna response
Ant. 1	4.26–10.68	-	Single-band
Ant. 2	5.85–7.43	6.27–6.78	Single-band
Ant. 3	4.92–7.29 8.41–10.52	6.44–7.13 -	Dual-band
Ant. 4	4.30–7.61 8.18–12.5	6.72–7.53 -	Dual-band
Ant. 5	2.29–3.21 4.22–13.23	5.83–6.49 9.91–10.8	Dual-band
Ant. 6	2.28–3.11 4.12–7.43 8.45–11.42	- 5.28–6.35 9.19–10.46	Triple-band

2.3. CP Mechanism

The simulated surface current distributions of the antenna at 5.8 GHz and 10.0 GHz are given in Figures 4(a) and (b) respectively to better explain the CP mechanism. As shown in Figure 4(a), it can be clearly seen that when ε_{reff}=0°, the direction of the resultant current vector at 5.8 GHz is lower-right. When ε_{reff} = 90°, the direction is upper-right. When ε_{reff} = 180°, the direction is upper-left. When ε_{reff} = 270°, the direction is lower-left. At 10.0 GHz, the direction of the resultant current vector changes in a similar way. So we can see that at different time instants ε_{reff} = 0°, 90°, 180°, 270°, the resultant current vector rotates in clockwise direction with the right-handed circular polarization (RHCP) at CP frequency bands.

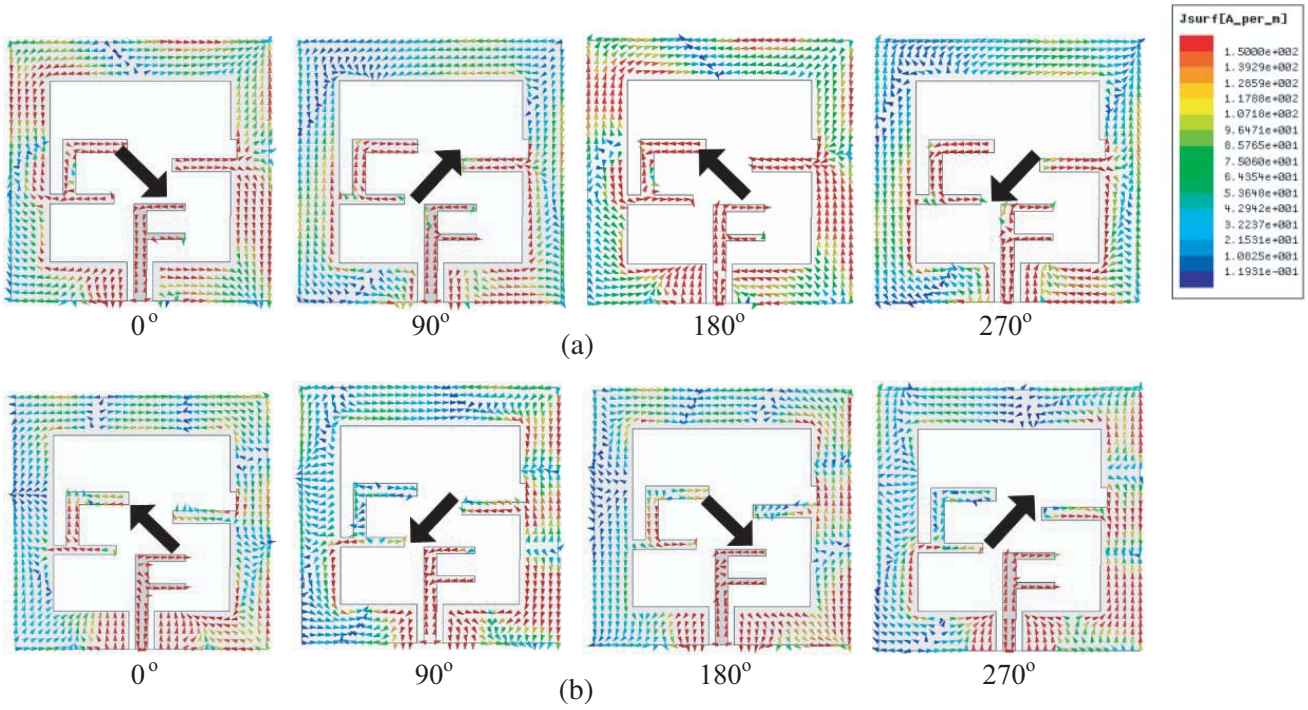

Figure 4. Simulated surface current distributions of the antenna. (a) At 5.8 GHz. (b) At 10 GHz.

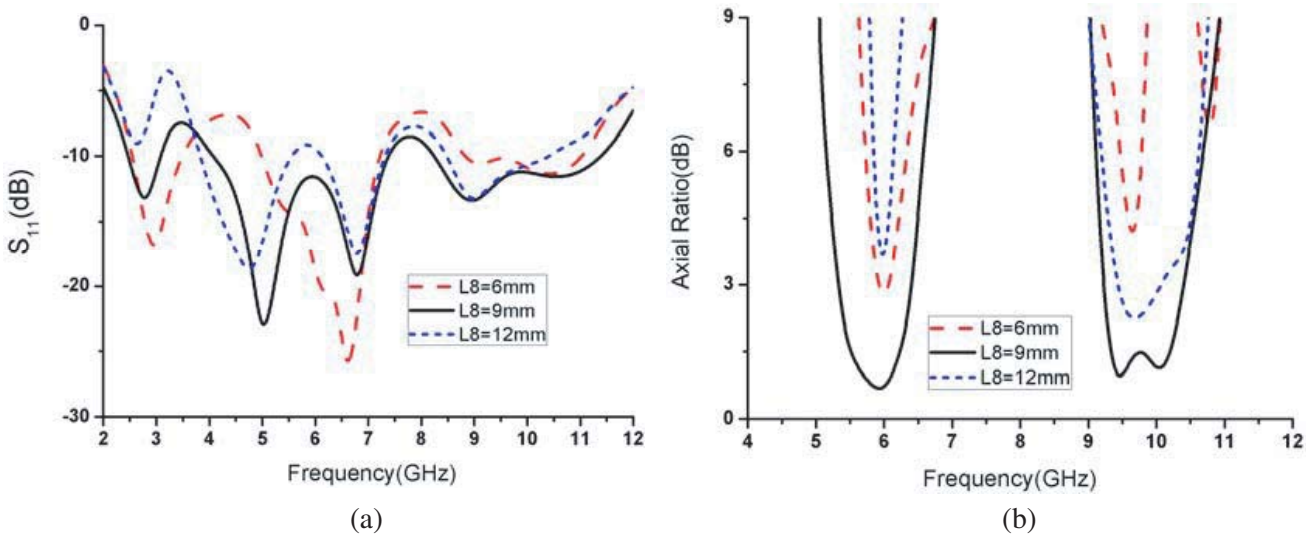

Figure 5. Simulated results of different values of L_8. (a) Reflection coefficient. (b) Axial ratio.

2.4. Parametric Study

In order to investigate the effects of the dimensions of the strips on the antenna, the simulated reflection coefficient and axial ratio against the frequency of the antennas with different values of L_8, L_f, and L_5 are given in Figures 5, 6, and 7, respectively. It can be observed from Figure 5(a) that the value of L_8 has larger influence on the lower operating band. The lower operating band decreases with the increase of L_8 while the higher operating band is nearly unchanged. As shown in Figure 5(b), the variation of L_8 has limited influence on AR performance. L_f has great influence on the middle operating band. From Figure 6(a), we can see that the middle operating band becomes better with the increase of L_f while the higher operating band is nearly unchanged. Also the AR performance of the middle operating band is greatly affected by the L_f. So we should choose the appropriate value $L_f = 15\,\text{mm}$. As shown in Figure 7, the variation of L_5 has great influence on the higher operating band at both impedance bandwidth and AR while the other bands are nearly unchanged.

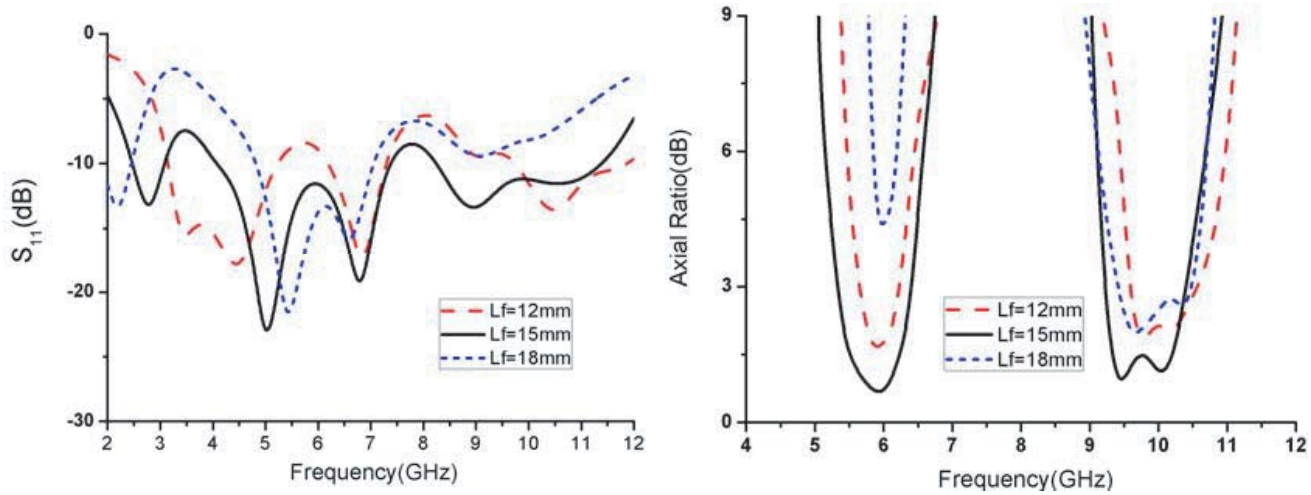

(a) (b)

Figure 6. Simulated results of different values of L_f. (a) Reflection coefficient. (b) Axial ratio.

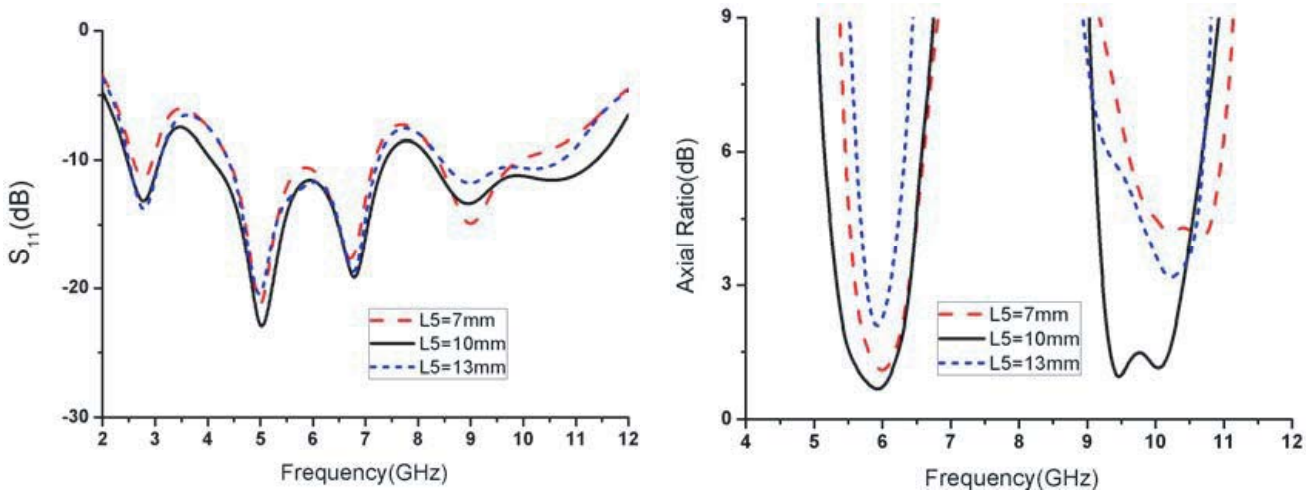

(a) (b)

Figure 7. Simulated results of different values of L_5. (a) Reflection coefficient. (b) Axial ratio.

3. FABRICATION AND MEASUREMENT RESULTS

To verify the design, the proposed antenna is fabricated and measured. A photograph of the prototype antenna is shown in Figure 8. Figure 9 shows photographs of the measured environment. S_{11} of the antenna is measured through an AV3672B vector network analyzer. The simulated and measured reflection coefficients (S_{11}) and the CP axial ratio (AR) against the frequency of the proposed antenna are shown in Figures 10(a) and (b), respectively. Good agreement between them can be observed. The measured 10-dB impedance bandwidths of the three separate operating bands are 830 MHz (2.28–3.11 GHz), 3.31 GHz (4.12–7.43 GHz), and 2.97 GHz (8.45–11.42 GHz), simultaneously covering the 2.4/5.2/5.8-GHz WLAN band and X-band. The 3-dB AR bandwidths are approximately 1070 MHz (5.14–6.21 GHz) and 860 MHz (9.46–10.32 GHz). It is observed that both CP bands are completely inside their respective impedance bands. The measured peak gains of the proposed antenna across the operation bands are shown in Figure 11, and stable gain variation can be observed. The measured and

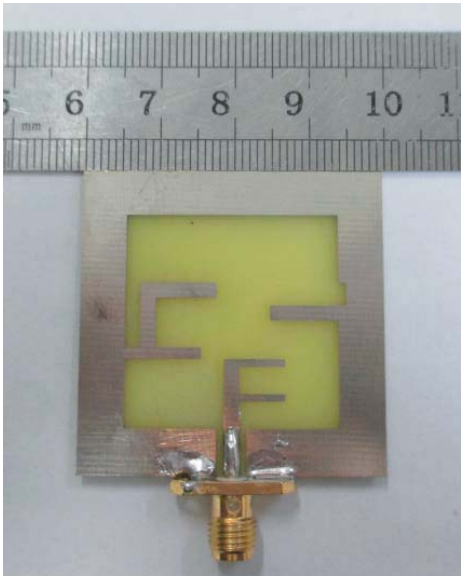

Figure 8. Photograph of the prototype antenna.

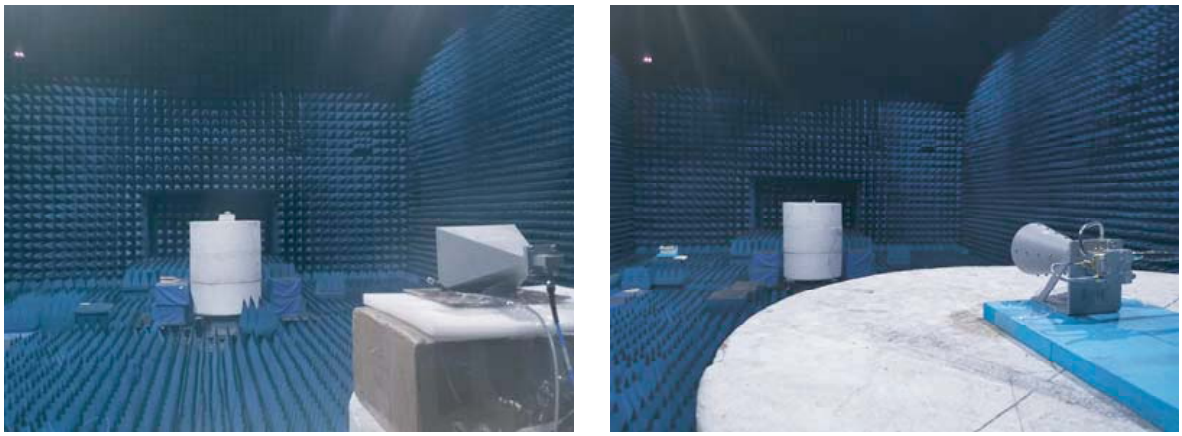

(a) (b)

Figure 9. Measurement setup for antenna measurement. (a) Linear polarization. (b) Circular polarization.

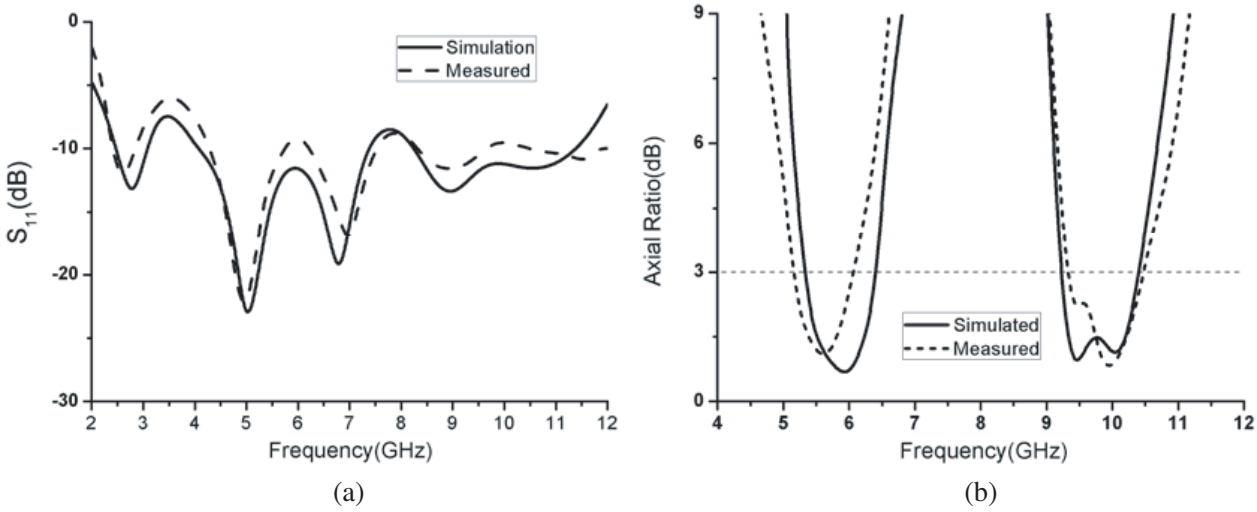

Figure 10. Simulated and measured results of the proposed antenna. (a) Reflection coefficient. (b) Axial ratio.

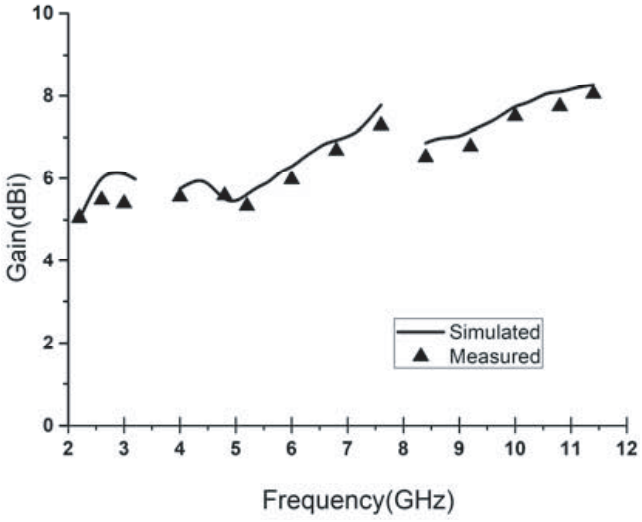

Figure 11. Simulated and measured gain of the proposed antenna.

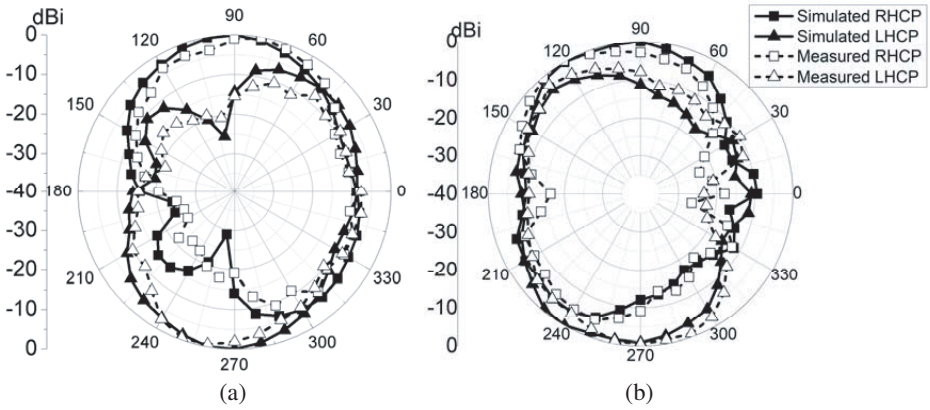

Figure 12. Simulated and measured radiation patterns of the proposed antenna. (a) 5.8 GHz. (b) 10 GHz.

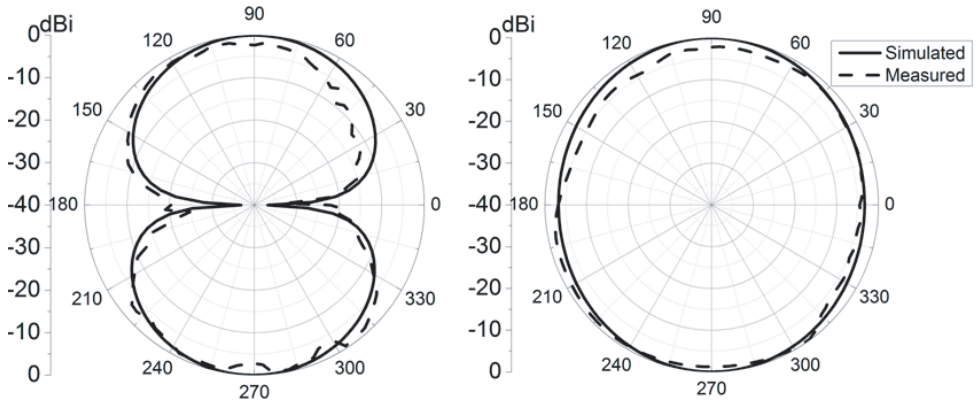

Figure 13. Measured and simulated radiation patterns for proposed antenna at 2.4 GHz. (a) E-plane. (b) H-plane.

simulated right-hand CP (RHCP) and left-hand CP (LHCP) radiation patterns at 5.8 GHz and 10 GHz are shown in Figure 12. For the linearly polarized band, the measured radiation patterns in the E-plane and H-plane at 2.4 GHz are shown in Figure 13. As shown in the figure, the antenna displays almost omnidirectional radiation in the H-plane and bidirectional radiation in the E-plane.

4. CONCLUSION

A compact tri-band coplanar waveguide (CPW)-fed patch antenna with dual-polarization characteristics is proposed. The antenna is simply composed of an F-shaped monopole antenna that is surrounded by a square slot ground plane. By inserting a crooked C-shaped strip and a rectangle strip with a slot opposite to the substrate at the center of the square slot ground, a wider impedance matching bandwidth is obtained. Meanwhile, two CP operation bands are obtained. By inserting a slot at the right of the square slot, a notched band centered at 5.5 GHz is achieved. The 10-dB impedance bandwidths of the three separate operating bands are 830 MHz (2.28–3.11 GHz), 3.31 GHz (4.12–7.43 GHz), and 2.97 GHz (8.45–11.42 GHz), simultaneously covering the 2.4/5.2/5.8-GHz WLAN band and X-band. The 3-dB AR bandwidths are approximately 1070 MHz (5.28–6.35 GHz) and 1270 MHz (9.19–10.46 GHz). It is observed that both CP bands are completely inside their respective impedance bands. In addition, the antenna is extremely simple and occupies small space. Moreover, almost monopole-like radiating pattern and stable gains across the three operating bands make such an antenna a good candidate in wireless application systems.

ACKNOWLEDGMENT

This work was supported in part by the Program for Talent of Colleges and Universities Service Enterprise of Xi'an under Grant 201805037YD15CG21(10), in part by the Program for Science and Technology Innovation of Xi'an University of Technology under Grant 103-451117003, in part by the Special scientific research project of Shaanxi Provincial Education Department under Grant 20JK0797, in part by the Natural Science Foundation of Shaanxi under Grant 2020JQ-653, in part by the Foundation of Key Laboratory of Antenna and Microwave Technology under Grant 61424020508192402013.

REFERENCES

1. Naser-Moghadasi, M., R. Sadeghzadeh, L. Asadpor, et al., "A small dual-band CPW-fed monopole antenna for GSM and WLAN applications," *IEEE Antennas & Wireless Propagation Letters*, Vol. 12, 508–511, 2013.

2. Shaw, T., D. Bhattacharjee, and D. Mitra, "Gain enhancement of slot antenna using zero-index metamaterial superstrate," *International Journal of RF & Microwave Computer Aided Engineering*, Vol. 27, No. 4, e21078, 2017.
3. Bai, H., G. M. Wang, and T. Wu, "High-gain wideband metasurface antenna with low profile," *IEEE Access*, Vol. 7, 177266–177273, 2019.
4. Kurra, L., M. Abegaonkar, A. Basu, et al., "FSS properties of a uni-planar EBG and its application in directivity enhancement of a microstrip antenna," *IEEE Antennas & Wireless Propagation Letters*, Vol. 15, 1606–1609, 2016.
5. Meriche, M. A., H. Attia, A. Messai, et al., "Gain improvement of a wideband monopole antenna with novel artificial magnetic conductor," *2016 17th International Symposium on Antenna Technology and Applied Electromagnetics (ANTEM)*, 2016.
6. Wang, N., Q. Liu, C. Wu, L. Talbi, Q. Zeng, and J. Xu, "Wideband Fabry-Perot resonator antenna with two complementary FSS layers," *IEEE Transactions on Antennas and Propagation*, Vol. 62, No. 5, 2463–2471, 2014.
7. Ge, Y., K. P. Esselle, and T. S. Bird, "A method to design dual-band,high-directivity EBG resonator antennas using single-resonant, singlelayer partially reflective surface," *Progress In Electromagnetics Research C*, Vol. 13, 245–257, 2010.
8. Tak, J., Y. Hong, and J. Choi, "Textile antenna with EBG structure for body surface wave enhancement," *Electronics Letters*, Vol. 51, No. 15, 1131–1132, 2015.
9. Hashmi, R. M. and K. P. Esselle, "Enhancing the performance of EBG resonator antennas by individually truncating the superstructure layers," *IET Microwaves Antennas & Propagation*, Vol. 10, No. 10, 1048–1055, 2016.
10. Chen, T. C. and C. Y. Tsai, "CPW-fed wideband printed dipole antenna for digital TV applications," *IEEE Transactions on Antennas and Propagation*, Vol. 59, No. 12, 4826–4830, 2011.
11. Ghobadi, A. and M. Dehmollaian, "A printed circularly polarized Y-shaped monopole antenna," *IEEE Antennas & Wireless Propagation Letters*, Vol. 11, 22–25, 2012.
12. Lacik, J., "Circularly polarized SIW square ring-slot antenna for X-band applications," *Microwave & Optical Technology Letters*, Vol. 54, No. 11, 2590–2594, 2012.
13. Saraswat, K., T. Kumar, and A. R. Harish, "A corrugated G-shaped grounded ring slot antenna for wideband circular polarization," *International Journal of Microwave & Wireless Technologies*, 1–6, 2020.
14. Hua, M. J., P. Wang, Y. Zheng, et al., "Compact tri-band CPW-fed antenna for WLAN/WiMAX applications," *Electronics Letters*, Vol. 49, No. 18, 1118–1119, 2013.
15. Chandra, K., M. Kumar, and M. D. Upadhayay, "Compact triple-band CPW-fed monopole antenna for bluetooth/WiMAX/WLAN applications," *Iranian Journal of Science and Technology — Transactions of Electrical Engineering*, No. 1, 2019.
16. Manouare, A. Z., S. Ibnyaich, D. Seetharamdoo, et al., "Design, fabrication and measurement of a novel compact triband CPW-fed planar monopole antenna using multi-type slots for wireless communication applications," *Journal of Circuits, Systems and Computers*, 2019.
17. Jo, G. J., S. M. Mun, D. S. Im, et al., "Novel design of a CPW-fed monopole antenna with three Arc-shaped strips for WLAN/WIMAX operations," *Microwave and Optical Technology Letters*, Vol. 57, No. 2, 268–273, 2015.
18. Iqbal, A., O. A. Saraereh, and S. K. Jaiswal, "Maple leaf shaped UWB monopole antenna with dual band notch functionality," *Progress In Electromagnetics Research C*, Vol. 71, 169–175, 2017.
19. Tao, J. and Q. Feng, "Compact UWB band-notch MIMO antenna with embedded antenna element for improved band notch filtering," *Progress In Electromagnetics Research C*, Vol. 67, 117–125, 2016.
20. Kamma, A., S. R. Gupta, G. S. Reddy, et al., "Multi-band notch UWB band pass filter with novel contiguous split rings embedded in symmetrically tapered elliptic," *Progress In Electromagnetics Research C*, Vol. 39, 133–148, 2013.

21. Yang, D., H. Zeng, S. Liu, et al., "A vivaldi antenna with switchable and tunable band-notch characteristic," *Progress In Electromagnetics Research C*, Vol. 68, 75–83, 2016.
22. Russo, I., L. Boccia, G. Amendola, and H. Schumacher, "Compact hybrid coaxial architecture for 3–10 GHz UWB quasi-optical power combiners," *Progress In Electromagnetics Research*, Vol. 122, 77–92, 2012.
23. Awan, W. A., N. Hussain, S. A. Naqvi, et al., "A miniaturized wideband and multi-band on-demand reconfigurable antenna for compact and portable devices," *International Journal of Electronics and Communications*, Vol. 122, 153266, 2020.
24. Chandra, K., M. Kumar, and M. D. Upadhayay, "Compact triple-band CPW-fed monopole antenna for bluetooth/WiMAX/WLAN applications," *Iranian Journal of Science and Technology — Transactions of Electrical Engineering*, Vol. 1, 1–7, 2019.
25. Pandit, Vivek, Kumar, "A compact CPW-fed tapered monopole triple-band antenna for WLAN/WiMAX application," *Microwave & Optical Technology Letters*, 2298–2303, 2018.
26. Mohammad Saadh, A. W. and R. Poonkuzhali, "A compact CPW fed multiband antenna for WLAN/INSAT/WPAN applications," *International Journal of Electronics and Communications*, Vol. 109, 128–135, 2019.